Electronic Supplementary Information (ESI)

Fabrication of Dog-Bone Shaped Au NR_{core}-Pt/Pd_{shell} Trimetallic Nanoparticles Decorated Reduced Graphene Oxide Nanosheets for Excellent Electrocatalysis

Soumen Dutta,[†] Chaiti Ray,[†] Anup Kumar Sasmal,[†] Yuichi Negishi,[‡] and Tarasankar Pal[†]*

[†] Department of Chemistry, Indian Institute of Technology, Kharagpur – 721302, India

[‡] Department of Applied Chemistry, Tokyo University of Science, Tokyo-1628601, Japan

E-mail: *tpal@chem.iitkgp.ernet.in*

Preparation of gold nanorods: Gold nanorods were prepared following the work from El-Sayed *et. al*.[S1] A typical seed mediated growth approach has been adopted with some minor modifications.[S2] A gold seed solution was first prepared by adding 0.6 mL of ice-cold $NaBH_4$ (0.01 M) to a vigorously stirred solution containing 10 mL $HAuCl_4$ (2.5×10^{-4} M) and CTAB (0.1 M). Then, the seed solution was kept at room temperature for 2 h to remove excess $NaBH_4$. Next, a growth solution was prepared by fully dissolving CTAB (0.4 mmol) in 40 mL of double distilled water followed by 2 mL of $HAuCl_4$ (0.01 M), 0.4 mL of $AgNO_3$ (0.01 M), 0.8 mL of HCl (1 M),[S3] and 0.32 mL of ascorbic acid (0.1 M) were added successively to the growth solution and mixed strongly until it became colorless. Then, 0.096 mL of the pre-synthesized gold seed solution was injected quickly into the growth solution and was left undisturbed at room temperature for overnight.

Preparation of graphene oxide (GO):

Graphene oxide (GO) was prepared from graphite powder following Hummer's method.[S4] In a beaker, 500 mg graphite flakes, 250 mg $NaNO_3$ and 12 mL conc. H_2SO_4 were stirred in an ice-bath. Then stepwise addition of 1.5 g solid $KMnO_4$ was performed into the above mixture so that the temperature remained below 20°C. After complete addition, the ice-bath was removed and the temperature rose to 35°C. The mixture was stirred for 30 minutes at this condition. During this aging the mixture turned out to be a paste after 20 minutes with small amount of gas evolution. After 30 minutes, 23 mL of distilled water added into the mixture which resulted in violent effervescence and the temperature was increased into 98°C. The diluted suspension, now brown in color, was maintained at this temperature for next 15 minutes. The suspension was then further diluted to 70 mL with warm water with subsequent treatment by 1.5 mL of 3% hydrogen peroxide to reduce the residual inorganic species.[S5] The resulted solution was then filtered hot in order to avoid precipitation. During filtration 0.5 M HCl was used to wash further in order to remove remaining salts. Furthermore, hot water washing was performed several times. Then it was centrifuged at 3500 rpm for 20 min to remove large particles. Finally the supernatant obtained was used as dispersion of GO in water. This dispersion was used for the synthesis of various composites in our study.

Instrumentation

Transmission electron microscopic (TEM) analyses of the samples were carried out on a Hitachi H-9000 NAR transmission electron microscope, operating at 200 kV. XRD was performed on a Bruker-AXS D8-Advance diffractometer with CuKα radiation (λ = 1.5418 Å) in the 2θ range of 5°–85° at a scanning rate of 0.5° min^{-1}. Fourier transform infrared (FTIR) studies were carried out with a Thermo-Nicolet continuum FTIR microscope. UV-visible absorption spectra were recorded with Thermo Scientific digital spectrophotometer. High-

angle annular dark-field scanning transmission electron microscopy (HAADF-STEM) image and elemental mapping analysis were performed in the UHR-FEG-TEM, JEOL JEM-2100F electron microscope using 200kV electron source. X-ray photoelectron spectroscopy (XPS) of the samples was done by ULVAC-PHI, Inc., Japan equipped with a microfocused (100 mm, 25 W, 15 kV) monochromatic AlKα beam. Raman spectra of the samples were recorded using a fiber-coupled micro-Raman spectrometer (Horiba Jobin Yvon Technology) equipped with 488 nm laser. Elemental compositions of synthesized samples were found by inductively coupled plasma-mass spectroscopy (ICP-MS) in Agilent 7500 instrument.

Electrochemical study: All electrochemical experiments were carried out on a CHI 660E electrochemical workstation. A standard three-electrode system was used for all electrochemical experiments, which consisted of a platinum wire as a counter electrode, standard calomel electrode (SCE) as reference electrode and a catalyst modified glassy carbon electrode (GCE) as the working electrode. The GCE was sequentially polished with alumina slurry (1.0, 0.3, and 0.05 μm) and rinsed carefully with double-distilled water. Then, the electrode was sonicated in water and finally in ethanol for 15 minutes. The GCE was then dried well at room temperature before use. To prepare the catalyst modified GCE, 7 μL of catalyst dispersion in water (1 mg/mL) was drop casted on GCE and dried at room temperature followed by 7 μL of 0.1% aqueous Nafion solution addition and dried well for 2 h. All electrochemical measurements were carried out at 22 ± 1 °C. Electrocatalytic activities of the catalysts were carried out in 0.5 M H_2SO_4, 1M ethyl alcohol and 1 M KOH mixture to compare their electrochemical properties at a scan rate 50 mV/s.

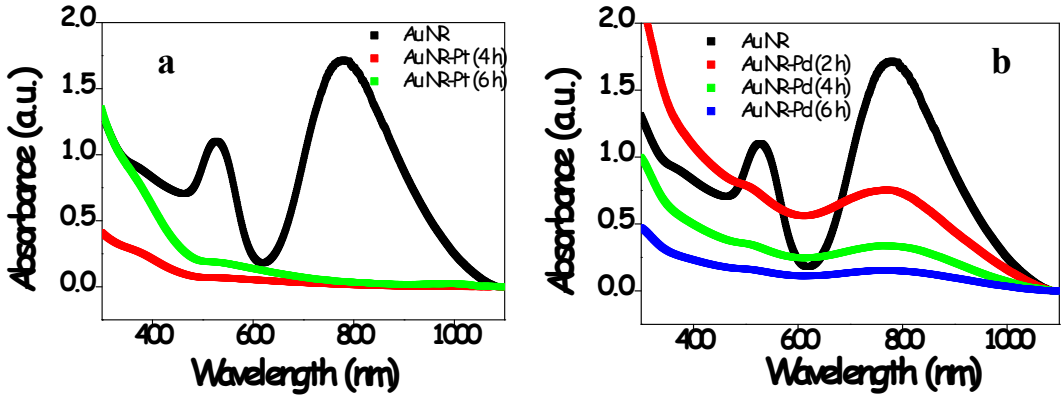

Figure S1. UV-vis spectra of bimetallic nanoparticles of (a) Au-Pt for GMT-1 fabrication and (b) Au-Pd for GMT-2 fabrication.

Gold nanorods clearly show two surface plasmon bands. Here transverse oscillation mode locates in the visible region at around 526 nm, while the other corresponding to the longitudinal oscillation mode between far-red and near-infrared (near-IR) region at 780 nm wavelength. The coverage of Pt NPs/Pd NPs on Au NRs has also been confirmed from UV-vis spectra of the resultant bimetallic particles as the signature spectral bands for Au NRs vanished completely with time.[S6]

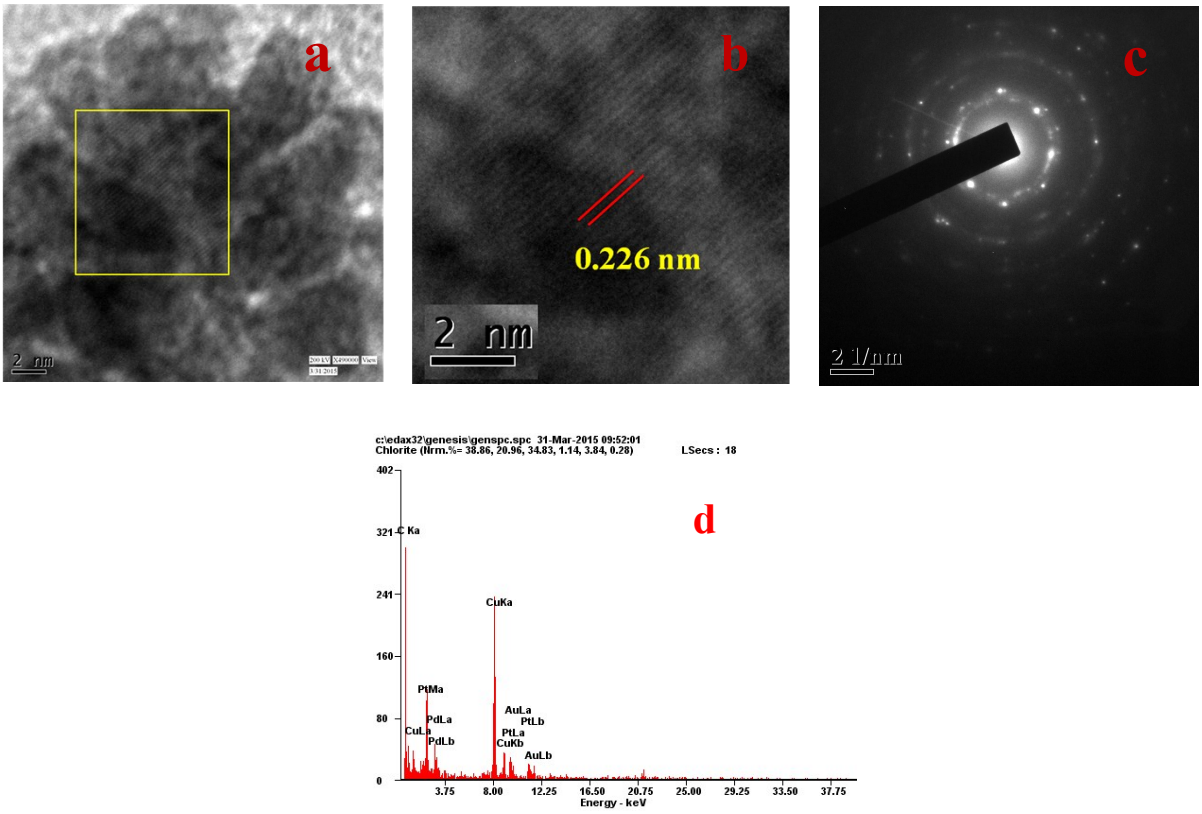

Figure S2. (a, b) HRTEM images of GMT-1. The indicated area has been considered for fringe spacing calculation. (c) SAED image and (d) EDAX spectra of GMT-1.

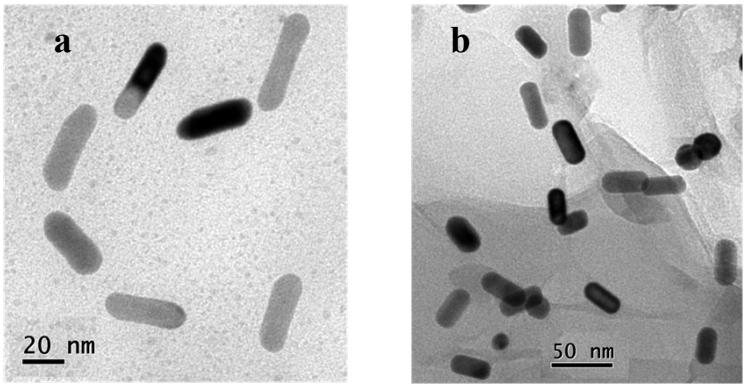

Figure S3. TEM images of (a) Au NRs and (b) Au-rGO.

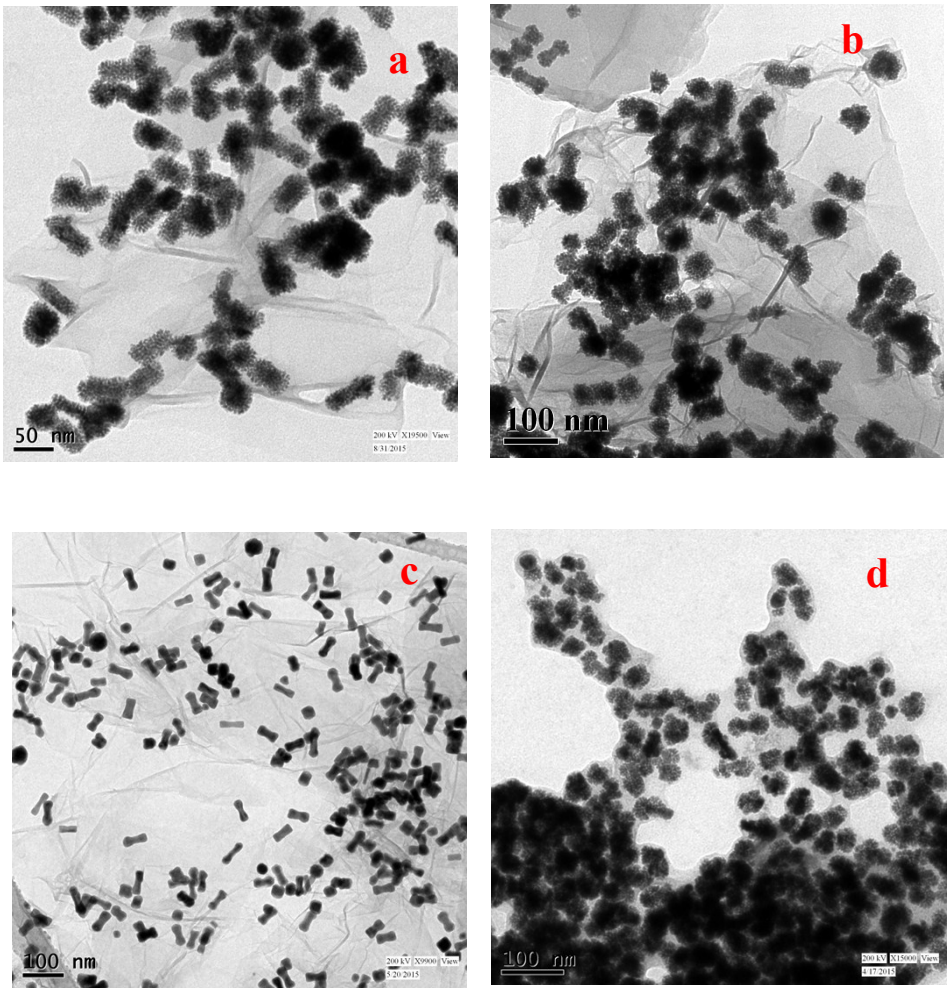

Figure S4. Low magnification TEM images of (a) Au-Pd-Pt-rGO **[GMT-2],** (b) Au-Pt-rGO **[GBT]**, (c) Au-Pd-rGO **[GBD]**, (d) Au-Pt-Pd **[TM]** nanocomposites.

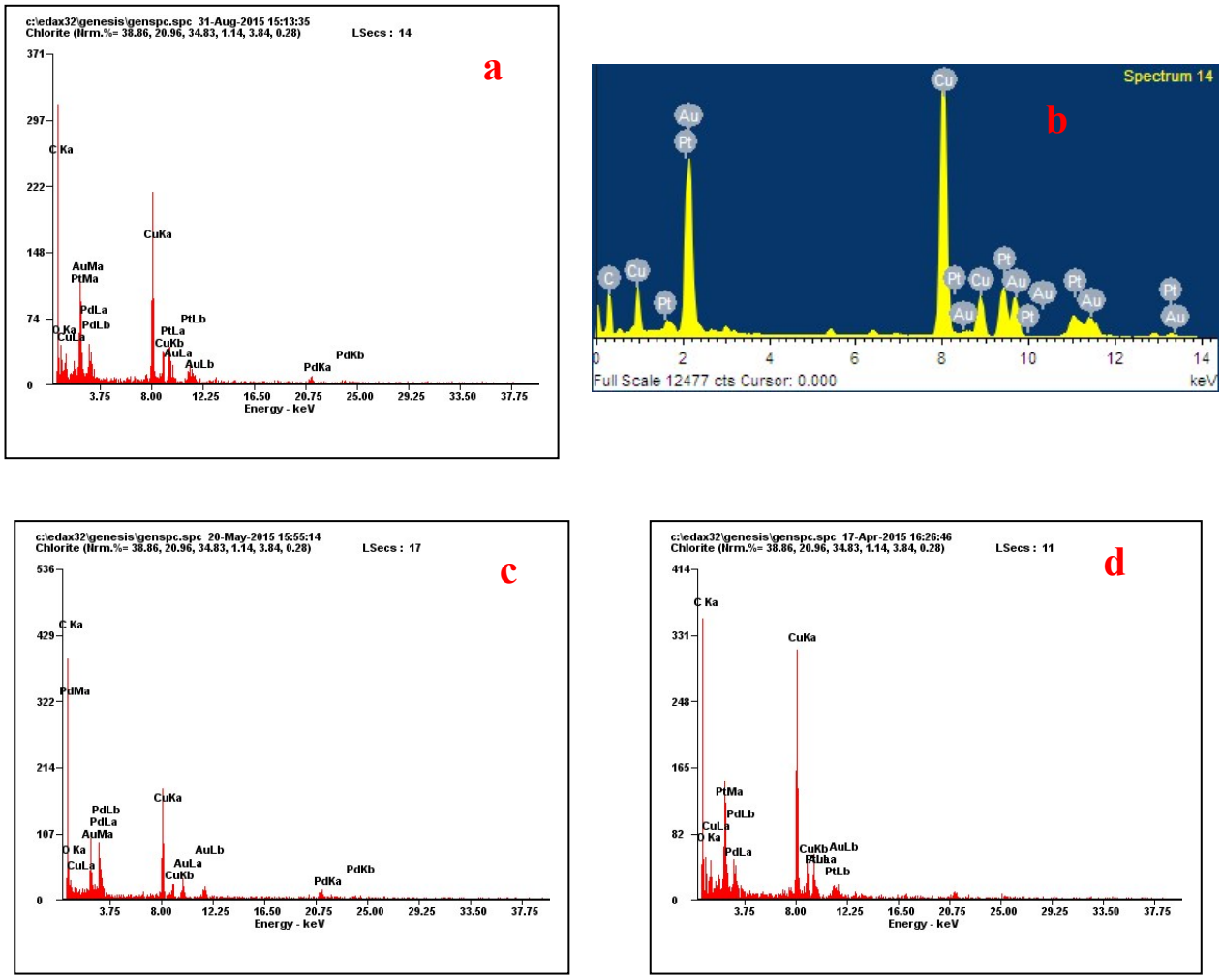

Figure S5. EDAX spectra of (a) Au-Pd-Pt-rGO **[GMT-2],** (b) Au-Pt-rGO **[GBT]**, (c) Au-Pd-rGO **[GBD]**, (d) Au-Pt-Pd **[TM]** nanocomposites.

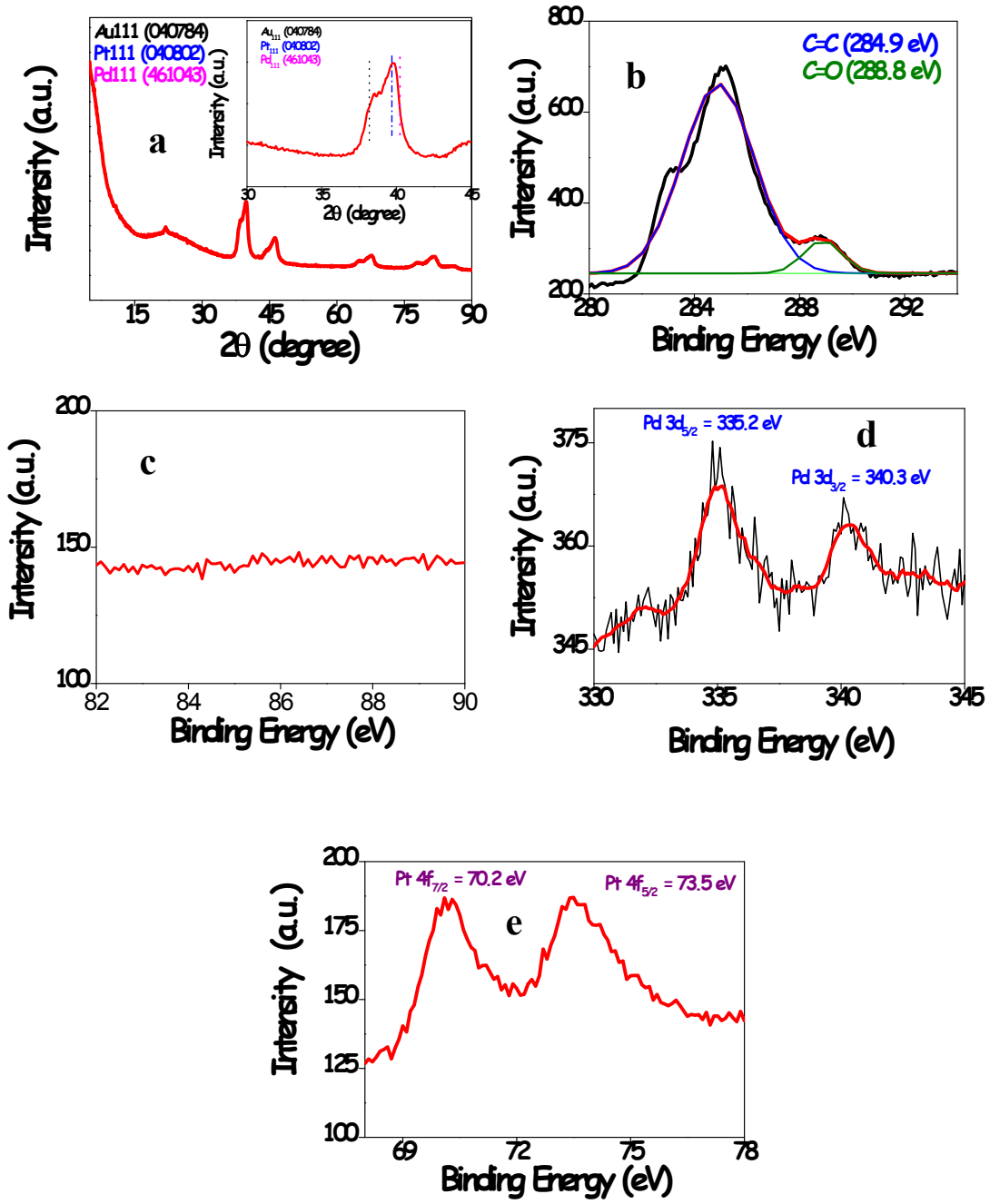

Figure S6. XRD pattern of GMT-2, XPS spectra for (b) C 1s, (c) Au 4f, (d) Pd 3d and (e) Pt 4f of GMT-2 nanocomposite.

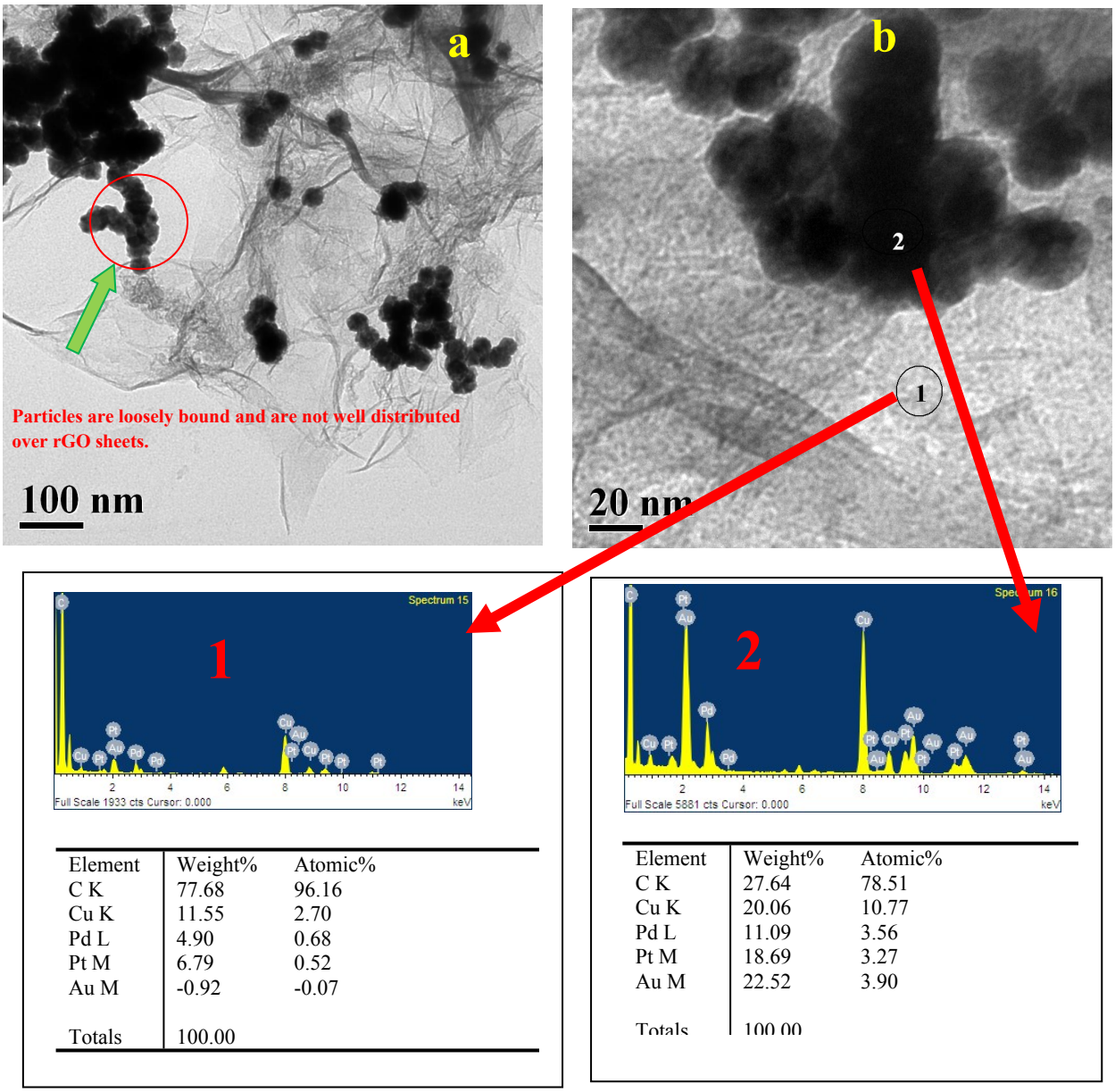

Figure S7. (a, b) TEM images and EDAX spectral data of GMTF.

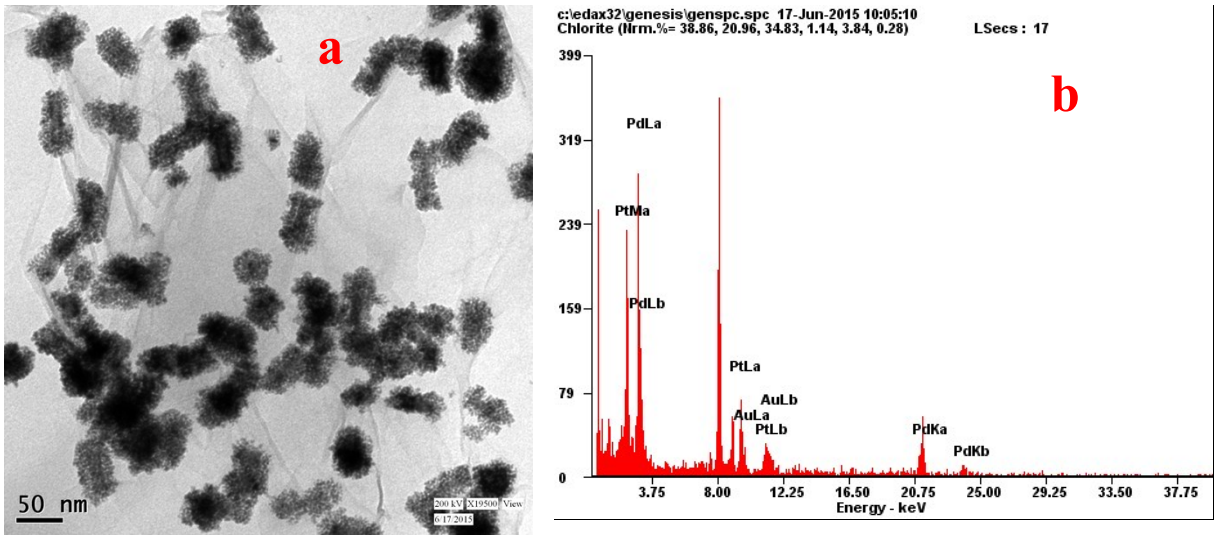

Figure S8. (a) TEM images and (b) EDX spectra of Au-Pt-Pd-rGO **[GMTB]** using ascorbic acid as reducing agent but in basic medium.

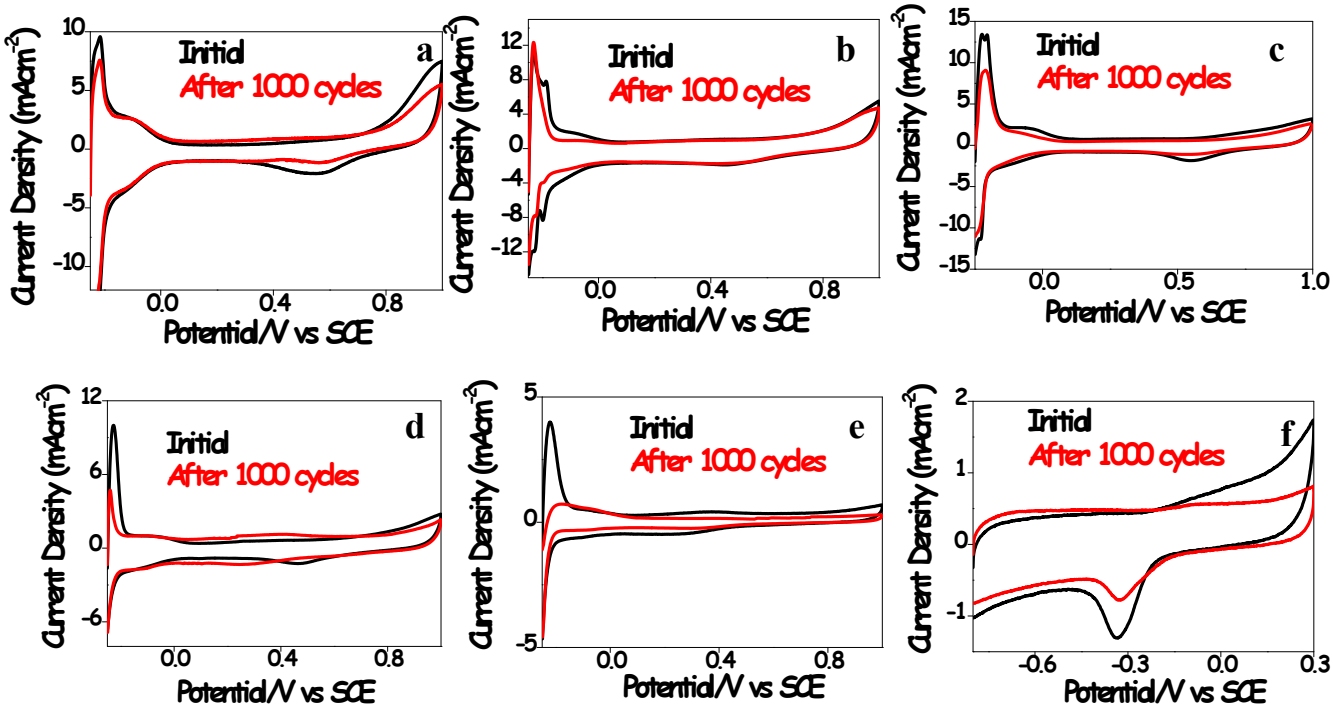

Figure S9. CV profiles in 0.5 M H_2SO_4 at 50 mV/s scan rate for (a) GMT-1, (b) GMT-2, (c) TM, (d) GBT, (e) commercial 20% Pt/C. (f) CV profiles in 1 M KOH for GBD. All the CV run have been performed at room temperature before and after 1000 EOR cycles.

Electrochemical active surface area (ECSA) was calculated considering area under the curve for hydrogen desorption in the region -0.25 to 0.1 V for Pt based catalysts such as GMT-1, GMT-2, GBT, TM and commercial Pt/C. Here the charge (Q_H) associated with the adsorbed hydrogen monolayer formation for standard Pt is considered as 210 μC cm^{-2}.[S7] Since Pd based catalyst (GBD) not stable in acid, ECSA measurement was done in KOH medium considering the peak area for metal oxide reduction. Standard charge associated for metal oxide reduction is 424 μC cm^{-2}. [S8] Here initial ECSA values are compared with the obtained result after 1000 accelerated EOR cycles.

Table S1. ICP-MS results for various nanocomposites.

Sample	Au (wt%)	Pd (wt%)	Pt (wt%)
GMT-1	3.75	8.48	26.96
GMT-2	4.41	12.21	23.43
TM	11.06	30.35	58.59
GBT	4.58	0	28.83
GBD	4.05	12.11	0

Table S2: Table for comparison on EOR activity with previously reported electrocatalysts.

Materials	Synthetic approach	Electrolyte solution	Electrocatalytic performances	Reference number
Corallite-like Pt–Pd alloy	$NaBH_4$ induced reduction of as-prepared $K_2PdCl_4/K_2Pt(CN)_4$ cyanogel	1.0 M ethanol + 0.5 M KOH	(i) Mass activity of 1075 $mAmg_{Pt}^{-1}$ (ii) 67% activity rentention after 2000 s of Chronoamperometry (CA) test	25
$Pd_{45}Pt_{55}$	Te NWs as a sacrificial template and reducing agent.	1 M ethanol + 0.5 M NaOH	Mass activity of 950 mA mg_{Pt+Pd}^{-1}	61
Au/Pd/Pt	Multistep procedure with galvanic replacement as the final step	1 M ethanol + 0.5 M NaOH.	Mass activity of 2.0 mA mg_{Pt}^{-1}	28
Pt-on-(Au@Pd) Trimetallic	Multistep procedure with seed medicated growth of first Pd then Pt on Au nanocube	0.5 M Ethanol + 0.1 M KOH	(i) Mass activity of 460 $mAmg_{Pt+Pd}^{-1}$ (ii) Stable for 300 EOR cycles	46
PtSnRh WNWs	Oleylamine and oleic acid assisted high temperature (190 °C) heating for 10 h	0.1 M ethanol + 0.1 M NaOH	(i) Onset potential at -0.5 V vs SCE (ii) Mass activity of 990 $mAmg_{Pt}^{-1}$	55
$Rh_{10}Pd_{40}Pt_{50}$	CTAC surfactant and citrtic acid as reducing agent for the metal ions on heating at 180°C for 1 h.	1.0 M ethanol +0.5 M KOH	(ii) Mass activity of 2600 $mAmg_{Pt}^{-1}$ (ii) 70% activity retention after 100 repeated cycles.	62
Pd_1Pt_1/C	Te nanowire as template which also participates in the galvanic displacement reaction with the noble metal ions	1 M ethanol + 0.5 M KOH	(i) Onset potential of -0.66 V vs SCE (ii) Mass activity of 936.6 mA mg_{Pd+Pt}^{-1} (iii) Activity increase at the initial cycles but decreases to 68% of the current after 1000 cycles.	26
Pt−Pd (1:3)/RGO	H_2 gas assisted reduction of the metal ions and GO	1 M ethanol + 1 M KOH	(i) Mass activity of 1486.7 mA m_{Pt+Pd}^{-1} (ii) 94% catalytic activity retention after 100 cycles.	48
porous PtPd NFs-RGO	Cytosine assisted reduction of precursors by hydrazine	1.0 M ethanol + 0.5 M KOH	Mass activity of 600 mA mg_{Pt}^{-1}	63
Pt-Pd nanocube/rGO	DMF assisted reduction with KI and PVP as structure-directing agent and capping agent	0.5 M ethanol + 1 M KOH	(i) Mass activity of 1920 $mAmg_{Pt}^{-1}$ (ii) 54% retention of activity after 500 EOR cycles.	64
rGO-Au@Pt	First rGO-Au from insitu reduction reaction by hydrazine, then GO-AuCu by CU UPD followed by galvanic recation between Cu and Pt^{4+}	0.5 M ethanol + 0.5 M NaOH	(i) Onset potential of -0.53 V vs Ag/AgCl (ii) Mass activity of 2446 $mAmg_{Pt}^{-1}$	65

Materials	Synthestic process	Electrolyte solution	Electrocatalytic performances	Reference number
Pt–Cu/RGO composites	Polyallylamine hydrochloride (PAH) as growth controlling agent and HCHO as reducing agent	1 M ethanol + 1 M KOH	(i) Onset potential 0.18 V vs RHE (ii) Mass activity of 1114.7mAmg$_{Pt}^{-1}$	47b
PdCu/3DGS	Hydrothermal treatment	1 M ethanol + 1 M KOH	(i) Onset potential -0.66 V vs Ag/AgCl (ii) Mass activity of 1140 mAmg$_{Pd}^{-1}$ (iii) Retention of 88% catalytic activity after 300 cycles	66
$Ni_1Pd_1Pt_1$/DNA-rGO	Stepwise growth and sodium borohydride mediated reduction	1 M ethanol + 0.5 M KOH	(i) onset potential at -0.5 V vs Hg/HgO (ii) Mass activity of 3400 mAmg$_{Pt}^{-1}$ (iii) Stable for 200 EOR cycles.	37
PdCo NTAs/CFC	template-assisted electrodeposition method	1 M ethanol + 1 M KOH	(ii) Mass activity of 1491 mAmg$_{Pd}^{-1}$ (iii) Activity retention of 90.6% after 500 EOR cycles.	67
Pt/PdCu/3DGF	Multistep procedures	1 M ethanol + 1 M KOH	(i) Onset potential at -0.6 V vs SCE (ii) Mass activity of 3000 mAmg$_{Pt+Pd}^{-1}$ (iii) 94% stability retention after 1000 cycles	36
Au/Ag/Pt hetero-nanostructures	Au NR as seed and ascorbic acid as reducing agents for the other metal ions.	1 M methanol + 1 M KOH	(i) Mass Activity of ~1000 mAmg$_{Pt}^{-1}$ (ii) Catalytic activity retention of 70% after 3000 cycles	16
Pt–Pd alloyed multipods	N-methylimidazole as a structure-directing agent and ethylene glycol (EG) as a solvent and a reducing agent	1.0 M KOH + 1.0 M EG	(i) Mass activity of 875 mAmg$_{Pt+Pd}^{-1}$ (ii) ~40 % catalytic activity retention after 2000 cycles.	7
G-AuPd@Pd	Good's buffers of 2-[4-(2 hydroxyethyl)-1-pipera-zinyl] ethanesulfonic acid (HEPES) as a reducing agent and a shape-directing agent	1.0 M KOH + 1.0 M methanol	(i) onset anodic potential is -0.46 V vs. Ag/AgCl (ii) Mass Activity of 650 mAmg$_{Pd}^{-1}$ (iii) 83% catalytic activity retention after 200 cycles	68
Pt–Pd nanodendrites	Poly(vinylpyrrolidone) (PVP) and urea were employed as the co-stabilizing and co-structure-directing agents during hydrazine mediated reduction of the metal ions followed by oriented attaachment	1.0 M KOH + 1.0 M methanol	(i) Mass Activity of 280 mAmg$_{Pt+Pd}^{-1}$ (ii) 50% activity retention after 500 cycles.	24
GMT-1	**Multistep ascorbic acid mediated reduction pathway**	**1.0 M KOH + 1.0 M ethanol**	**(i) Onset potential -0.68 V vs SCE** **(ii) Mass activity of 3127.83 mAmg$_{Pt}^{-1}$ (2337.8 mAmg$_{Pt+Pd}^{-1}$)** **(iii) 86.3 % catalytic activity retention after 1000 cycles**	**This work**
GMT-2	**Multistep ascorbic acid mediated reduction pathway**	**1.0 M KOH + 1.0 M ethanol**	**(i) Onset potential -0.69 V vs SCE** **(ii) Mass activity of 3806.7 mAmg$_{Pt}^{-1}$ (2499.7 mAmg$_{Pt+Pd}^{-1}$)** **(iii) 77.1 % catalytic activity retention after 1000 cycles**	**This work**

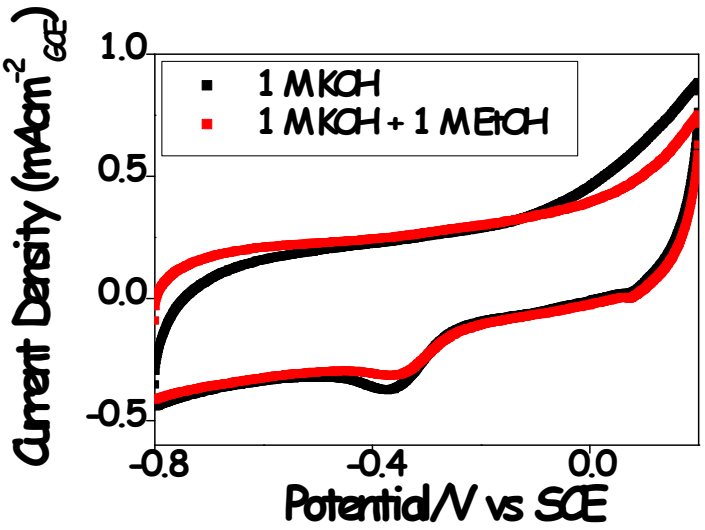

Figure S10. CV profile for Au-rGO (GMU) with two electrolyte solutions (1 M KOH and mixture of 1 M KOH + 1 M EtOH).

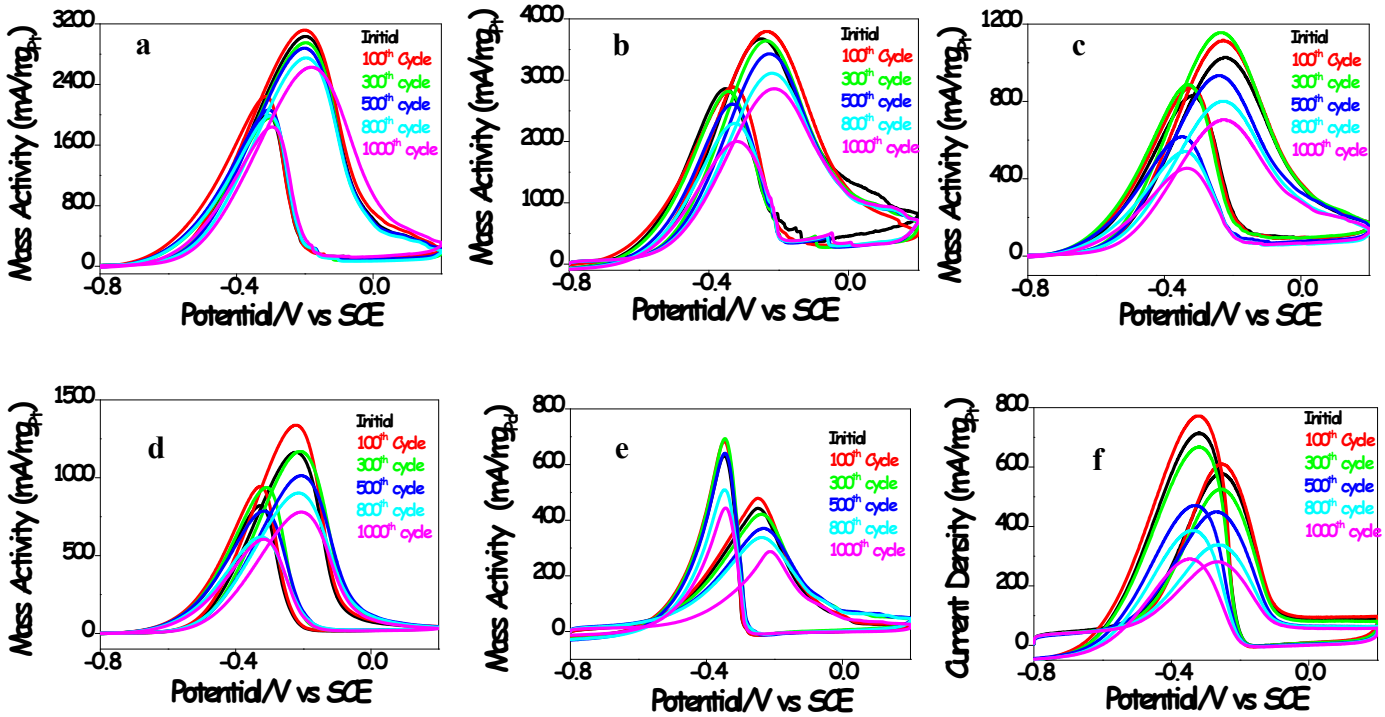

Figure S11. Change of mass activity with respect to cycles for (a) GMT-1, (b) GMT-2 (c) GBT, (d) TM, (e) GBD, (f) Pt/C.

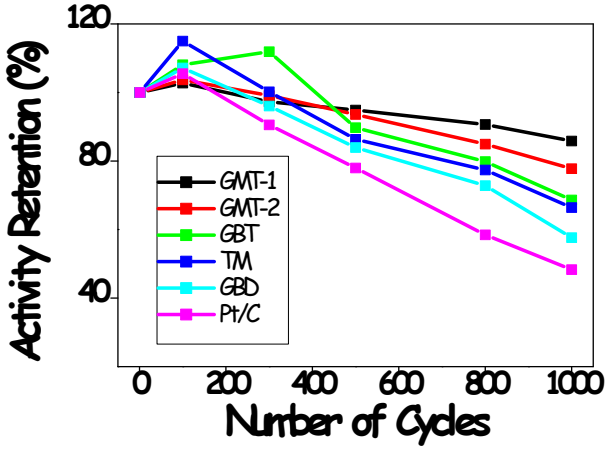

Figure S12. Activity retention for various catalysts with number of cycles.

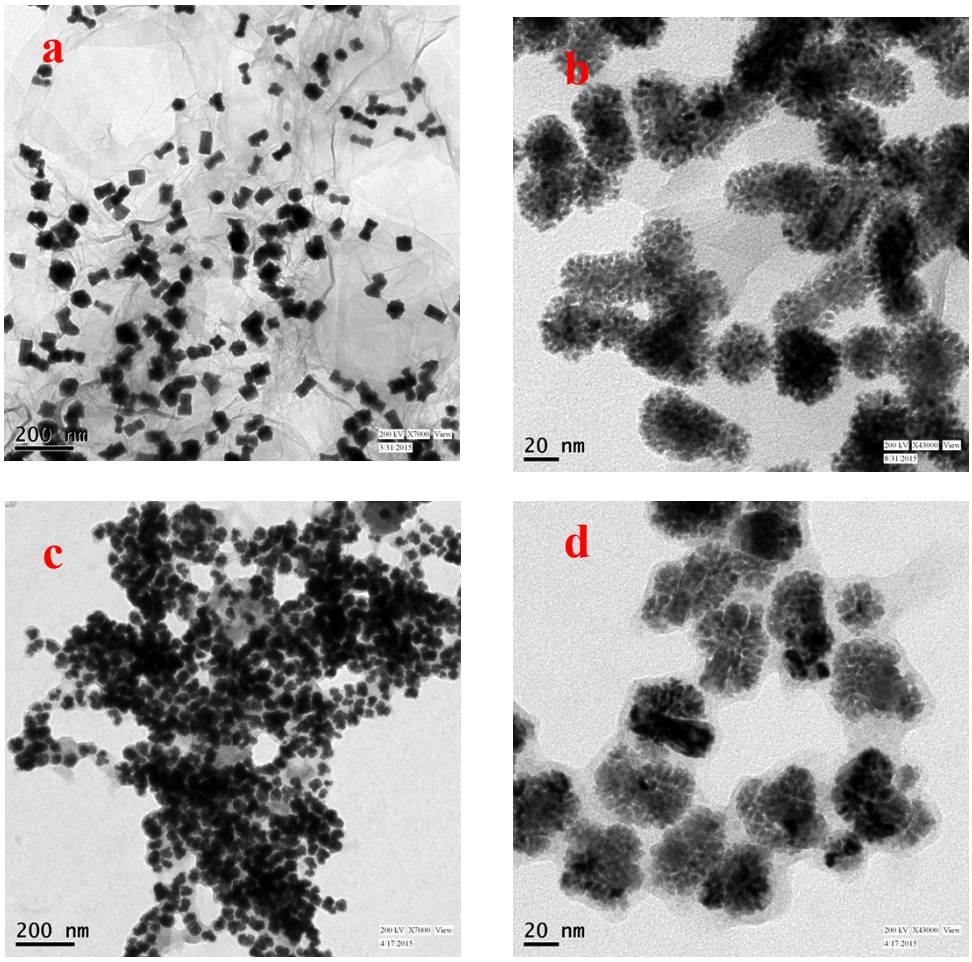

Figure S13. TEM images of (a) GMT-1, (b) GMT-2, (c, d) TM after 1000 accelerated EOR cycles.

After 1000 EOR cycles, the trimetallic particles in case of GMT-1 are still distinct, but in other cases they are highly aggregated. Compared to TM, GMT-2 has less association of the particles which may be due to the presence of rGO support.

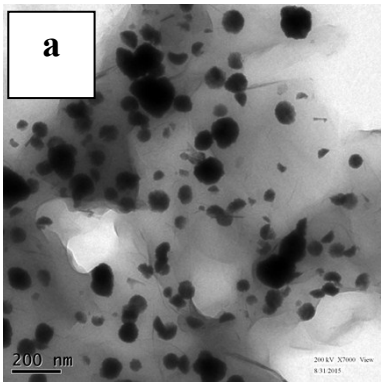

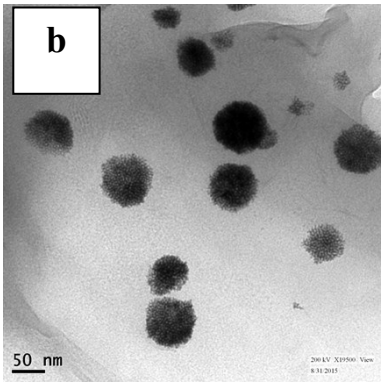

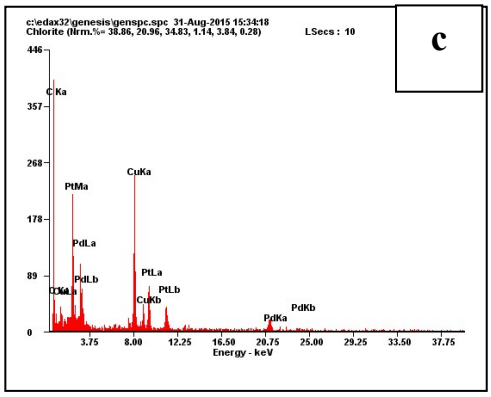

Element	Wt %	At %
PtM	59.30	45.68
PdL	34.96	49.38
PtL	04.93	03.79
PdK	00.81	01.14

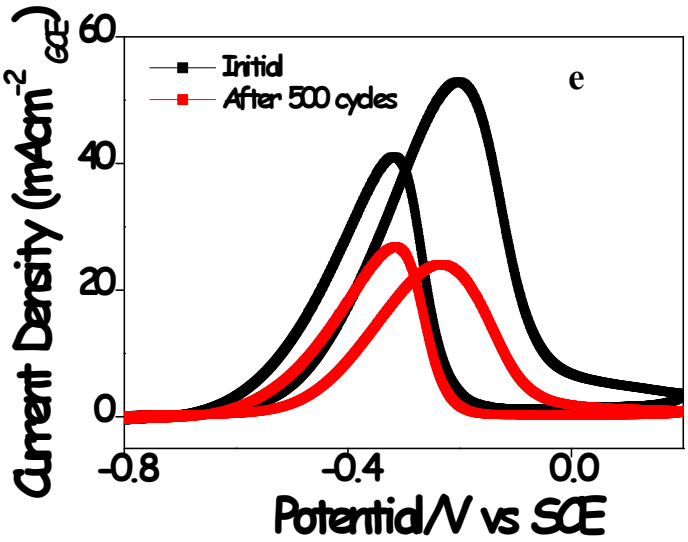

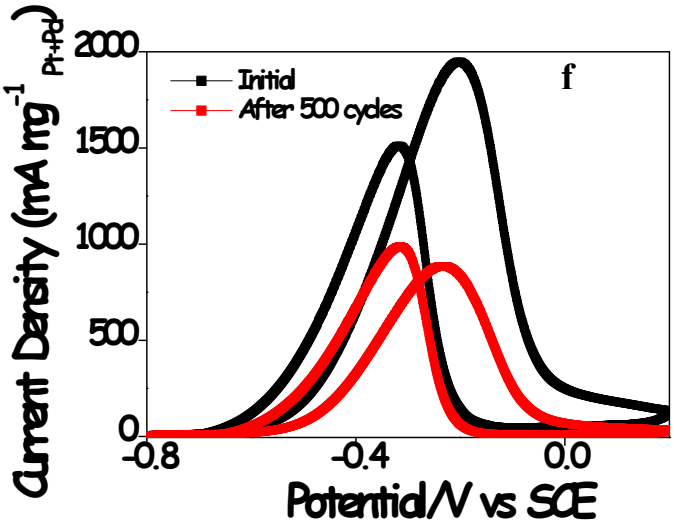

Figure S14. (a, b) TEM images of Pd-Pt-rGO (PPG) synthesized from the same adopted method but in absence of Au NRs. (c) EDAX spectra and spectral results of PPG, (d) ICP

results of PPG, (e) CV profile and (f) mass activity value with respect to total mass of Pd and Pt towards EOR with PPG catalyst. The obtained mass activity value is 1950.1 mA mg_{Pt+Pd}^{-1}.

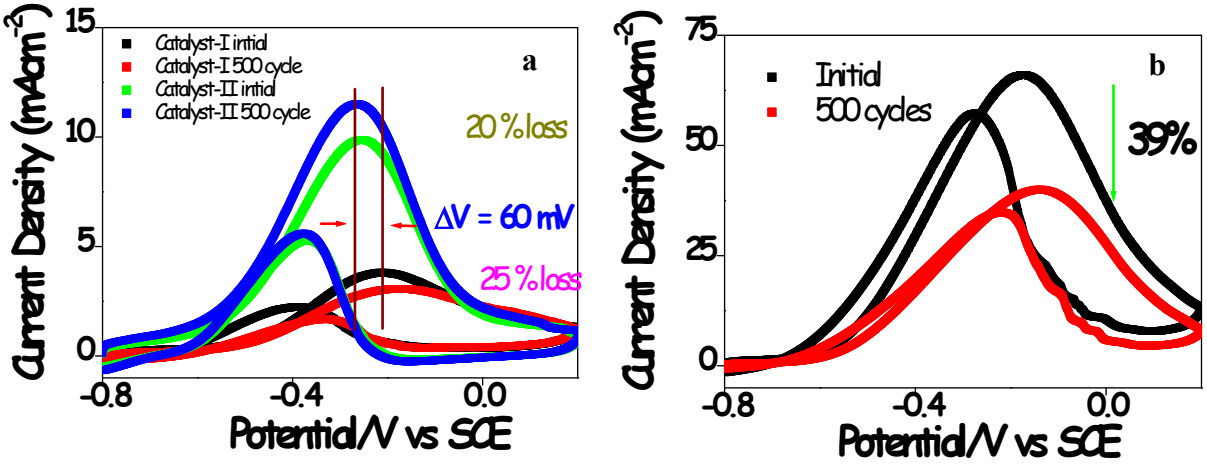

Figure S15. (a) CV profiles for EOR with 2 sets of GMTF catalyst. (b) CV profiles for EOR with GMTB catalyst.

For GMTF we found maximum 11.6 and 3.8 $mAcm^{-2}$ current density during EOR. The CV results for GMTF are not consistent at all. However, 3-4 sets of GMT catalysts results in almost same results but GMTF they varied enormously. This is due to their irregular morphology. Three metals in GMTF are not acted as unit like GMT case; rather they perform individually which creates the observed disorder.

In GMTB the observed current density (~67 $mAcm^{-2}$) is quite close with the GMT but its lower stability comes from the overgrowth of the particles in certain cases causing agglomeration.

REFERENCES:

S1. B. Nikoobakht and M. A. El-Sayed, *Chem. Mater*., 2003, **15,** 1957-1962.

S2. L. N. Kong, W. Chen, D. K. Ma, Y. Yang, S. S. Liu and S. M. *J. Mater. Chem*., **2**012, **22,** 719−724.

S3. T. Zhao, K. Yu, L. Li, T. Zhang, Z. Guan, N. Gao, P. Yuan, S. Li, S. Q. Yao, Q.-H. Xu and G. Q. Xu, *ACS Appl. Mater. Interfaces,* 2014, **6,** 2700−2708.

S4. W. S. Hummers and R. E. Offeman, *J. Am. Chem. Soc*., 1958, **80,** 1339.

S5. S. K. Bhunia and N. R. Jana, *ACS Appl. Mater. Interfaces,* 2011, **3,** 3335–3341.

S6. G.-R. Zhang, J. Wu and B.-Q. Xu, *J. Phys. Chem. C,* 2012, **116,** 20839−20847.

S7. Z. Huang, H. Zhou, Z. Chen, F. Zeng, L. Chen, W. Luo, and Y. Kuang, *Electrochim. Acta,* 2014, **147,** 643–649.

S8. R. Jiang, D. T. Tran, J. P. McClure and D. Chu, *ACS Catal.,* 2014, **4,** 2577-2586.